


# MiR-339-5p Inhibits Ferroptosis by Promoting Autophagic Degradation of FTH1 Through Targeting ATG7 in Liver Cancer Cells

Fei Cao, Weiyuan Hao, Weiren Liang, Hui Zeng and Jiaping Zheng 

Department of Interventional Therapy, Zhejiang Cancer Hospital, Institute of Basic Medicine and Cancer (IBMC), Chinese Academy of Sciences, Hangzhou, China.

Clinical Medicine Insights: Oncology  
Volume 18: 1–9  
© The Author(s) 2024  
Article reuse guidelines:  
sagepub.com/journals-permissions  
DOI: 10.1177/11795549241244783



## ABSTRACT

**BACKGROUND:** Liver cancer has a high incidence and mortality rate worldwide, and there is an urgent need to identify new therapeutic strategies and predictive targets to improve the clinical outcomes of advanced liver cancer. Ferroptosis holds promise as a novel strategy for cancer therapy. Epigenetic dysregulation is a hallmark of cancer, and noncoding RNAs are tightly involved in cell fate determination. Therefore, we aimed to identify a novel ferroptosis regulator from aberrantly expressed microRNAs that may serve as a novel biomarker and therapeutic target for liver cancer.

**METHODS:** The expression signature and prognostic value of miR-339 was assessed using TCGA data set. The role of miR-339/ATG7/FTH1 axis in liver cancer cells were evaluated through growth curve, colony formation, 7-AAD staining. The role of miR-339 in regulation of ferroptosis was determined by immunofluorescence staining, flow cytometry, and Elisa kits.

**RESULTS:** Here, we showed that miR-339 is aberrantly overexpressed in patients with liver cancer. In addition, miR-339 inhibition dramatically suppresses liver cancer progression. Furthermore, miR-339 silencing drives cell death and inhibits liver cancer progression, indicating that miR-339 may serve as a novel ferroptosis suppressor. Mechanistically, we demonstrated that miR-339 targets ATG7 to facilitate the autophagic degradation of FTH1 and prevent ferroptosis in liver cancer cells.

**CONCLUSIONS:** We provide important evidence that the miR-339 inhibition activates of the autophagy pathway to promote ferroptosis by degrading FTH1 in liver cancer cells. We found that miR-339 regulates the balance between ferroptosis and autophagy in liver cancer cells.

**KEYWORDS:** Liver cancer, miR-339-5p, ferroptosis, ATG7, autophagy

**RECEIVED:** July 6, 2023. **ACCEPTED:** March 15, 2024.

**TYPE:** Interventional Treatment of Hepatocellular Carcinoma (HCC) – Original Research Article

**FUNDING:** The author(s) disclosed receipt of the following financial support for the research, authorship, and/or publication of this article: This research was financially supported by the Medicine Health Science and Technology Project of Zhejiang Province (2023KY600) and the Medicine Health Science and Technology Project of Zhejiang Province (2022KY118).

**DECLARATION OF CONFLICTING INTERESTS:** The author(s) declared no potential conflicts of interest with respect to the research, authorship, and/or publication of this article.

**CORRESPONDING AUTHOR:** Jiaping Zheng, Department of Interventional Therapy, Zhejiang Cancer Hospital, Institute of Basic Medicine and Cancer (IBMC), Chinese Academy of Sciences, Hangzhou 310022, China. Email: zhengjp\_2013@126.com

## Introduction

Liver cancer has a high incidence and mortality rate worldwide and seriously threatens people's lives and health.<sup>1–3</sup> Unfortunately, patients with early-stage liver cancer are generally insensitive to radiotherapy, and systemic therapies for patients with advanced liver cancer have limited clinical benefits, resulting in a low 5 year survival rate. Resistance to the first-line clinical drug sorafenib for advanced liver cancer treatment has also emerged over short periods of time,<sup>4–6</sup> highlighting the urgent need to identify new therapeutic strategies and predictive targets to improve the clinical benefits for advanced liver cancer.

Cancer cell death is critical for the clearance of tumor cells.<sup>7</sup> Ferroptosis is a form of regulated cell death mediated by iron-catalyzed lipid peroxidation.<sup>8</sup> Recent studies have shown that the unique regulatory mechanism of ferroptosis holds promise as a novel strategy in cancer therapies.<sup>9,10</sup> Tumor cells resist ferroptosis through 3 pathways: limiting cellular peroxidation, limiting the pool of unstable iron, and upregulating their own ferroptosis defense systems to promote tumorigenesis and metastasis.<sup>9,11,12</sup>

Ferroptosis is one of the reasons why liver cancer cells are resistant to targeted drugs, highlighting the potential of novel ferroptosis sensitizers as a promising therapeutic modality for liver cancer treatment.<sup>5,9,13,14</sup>

Autophagy is an evolutionarily conserved degradation pathway that maintains homeostasis.<sup>15</sup> The classical pathway of ferroptosis is induced by inactivating the cell membrane's primary protective mechanism against peroxidative damage, whereas the nonclassical ferroptosis signaling pathway is initiated by increasing the "unstable iron pool."<sup>7</sup> Autophagy-related (ATG) genes play a central role in regulating autophagy.<sup>16</sup> ATG7 plays an essential role in the formation of autophagosomes.<sup>16</sup> Recent studies have shown that ATG5/ATG7 can promote ferroptosis by degrading the iron transport protein FTH1.<sup>17</sup> However, regulatory mechanisms underlying the crosstalk between ferroptosis and autophagy in liver cancer remain largely unknown.

Epigenetic dysregulation is a hallmark of the development of cancer.<sup>18</sup> MicroRNAs (miRNAs), an important component of epigenetics, are noncoding RNAs with a length of approximately 22 nucleotides that regulate gene expression by binding to



complementary target mRNA sequences to recognize and inhibit the translation or stability of the target mRNA, eventually inhibiting protein synthesis.<sup>19</sup> MicroRNAs play vital roles in disease and tumor development.<sup>20,21</sup> MicroRNAs have been found to be aberrantly expressed in a variety of tumor tissues, such as breast, colon, liver, and ovarian cancers and are potential cancer treatment targets.<sup>20,22-25</sup> Among these miRNAs, miR-339 is an miRNA that is highly evolutionarily conserved and has been found to play a role in regulating physiological processes such as tumor cell proliferation and metastasis in breast, colorectal, and gastric cancers.<sup>24-26</sup> However, its exact functions and mechanisms in the progression of liver cancer remain unclear. Previous studies have shown that miR-339 regulates ferroptosis by targeting SLC7A11 in lung cancer.<sup>27</sup> Guan et al found that miR-339 regulates drug resistance in laryngeal cancer cells via autophagy.<sup>28</sup> These findings support our hypothesis that miR-339 is a key regulator of the crosstalk between autophagy and ferroptosis.

Here, we found that miR-339 was aberrantly upregulated and promoted the proliferation and metastasis of liver cancer cells by inactivating ferroptosis. In addition, target prediction suggested that miR-339 may be critical for governing the crosstalk between autophagy and ferroptosis to regulate liver cancer progression. In this study, we aimed to elucidate the role of miR-339 in liver cancer progression and demonstrate the underlying mechanism.

## Methods

### *Cell culture and reagents*

Human liver cancer cells HepG2 were obtained from the American Type Culture Collection (ATCC). HCCC9810 was obtained from Procell (Catalog, CL-0095). Cell cultures were grown in Dulbecco's Modified Eagle's Medium (DMEM) (Gibco, Grand Island, NY, USA) with 10% fetal bovine serum (FBS) (EallBio, Beijing, China; # 03. U16001) at 37°C in a humidified atmosphere of 95% air and 5% CO<sub>2</sub>. RSL3, dimethyl sulfoxide (DMSO), Z-VAD-FMK, necrosulfonamide, and ferrostatin-1 were purchased from MedChemExpress (MCE, Monmouth Junction, NJ, USA).

### *Bioinformatic analysis*

The expression pattern of miR-339 and the correlation between its expression and clinical outcome of patients with liver cancer were generated by searching has-mir-339 in the UALCA website (<https://ualcan.path.uab.edu/cgi-bin/ualcan-res.pl>). The "Liver hepatocellular carcinoma" data set in TCGA was included in these analyses.

### *The correlations between individual gene and pathway score*

The clinical information and expression profiles at level 3 obtained from the TCGA data set for liver hepatocellular carcinoma (LIHC) were downloaded. The analysis was carried

out using the R GSVA package with the selected parameter of "method = 'ssgsea'." The relation between gene scores and pathway scores was examined using Spearman's correlation. All R packages and analysis techniques were applied in R version 4.0.3. A significance level of  $P < .05$  was considered.

### *RNAi transfection*

Cells were plated to 50% confluency and transfected with shATG7 oligonucleotides 5'-CCGGCCTGAACAGAATCATCCTTA ACTCGAGTTAAGGATGATTC TGTTCAGGTTTTTTG-3' or nontargeting shRNA or 200 nM miR-339-5p inhibitor (5'-CGUGAGCUCCUGGAGGACAGGGA-3') or inhibitor-negative control (5'-CAGUACUUUGUGUAGUACAA-3') by Lipofectamine 2000 (Invitrogen, Carlsbad, CA, USA) in Opti-MEM (Invitrogen), according to the manufacturer's protocol.

### *Real-time quantitative polymerase chain reaction*

Total cellular RNAs were extracted using TRIzol reagent (Invitrogen) and quantified. The RNA was then reverse-transcribed to cDNA using the RevertAid Reverse Transcriptase. Quantitative polymerase chain reaction was performed using FastStart Universal SYBR Green Master (Rox) from Roche (Basel, Switzerland), according to the manufacturer's instructions, and the mRNA levels were normalized to the actin and miRNA levels to the U6 level. The primer sequences used for real-time quantitative polymerase chain reaction (RT-qPCR) analyses are listed as follows:

Human-ATG7: 5'-ACC CGG CTC ACC CTG GTT TGT-3' and 5'-ACC CCA GTC CTG TAG GTG TGC TG-3'.

Human-miR-339-5p: 5'-GTC GTA TCC AGT GCG TGT CGT GGA GTC GGC AAT TGC ACT GGA TAC GAC CGT GAG CTC-3' (a stem-loop primer); 5'-GGG TCC CTG TCC TCC A-3' (forward); 5'-TGC GTG TCG TGG AGT C-3' (reverse).

Human-actin: 5'-CAC CAT TGG CAA TGA GCG GTT C-3' and 5'-AGG TCT TTG CGG ATG TCC ACG T-3'.

U6: 5'-CTC GCT TCG GCA GCA CA-3' and 5'-AAC GCT TCA CGA ATT TGC GT-3'.

### *Colony formation assays*

The cells were seeded in 6-well plates for a minimum of 14 days. The cells were transfected with the indicated inhibitors and the medium was replaced every 3 days until visible colonies formed. The cells were fixed using 4% paraformaldehyde for a duration of 20 minutes. Following this, they were stained with 0.5% crystal violet for a period of 30 minutes. Finally, the cells were left to dry overnight.

### *Transwell assay*

For the *in vitro* migration assay, an 8  $\mu\text{m}$  pore size Boyden chamber (Corning Costar, Cambridge, MA, USA) was used. Specifically, cells ( $200\ \mu\text{L}$ ,  $1 \times 10^5$ ) were seeded in the upper chamber of the Boyden chamber in serum-free DMEM, whereas  $500\ \mu\text{L}$  of 10% FBS was added to the DMEM in the lower chamber to act as a chemoattractant. Following a 12 hour incubation period, the cells located on the upper side of the filter were carefully removed, leaving behind only the cells that had migrated to and adhered to the underside of the membranes. These remaining cells were then fixed using methanol and stained with crystal violet for visualization purposes. Subsequently, the migrating cells were counted under a microscope. To ensure a representative number of cells were accounted for, 5 contiguous fields of each sample were meticulously examined using a  $20\times$  objective for a thorough analysis of the cells that successfully migrated across the membrane.

### *Cell death assays*

Liver cancer cells were seeded at a density of  $2 \times 10^5$  cells per well in 6-well tissue culture plates. The cells were transfected with the indicated inhibitors, collected, and washed with phosphate-buffered saline (PBS). To measure cell death, cells stained with  $5\ \mu\text{g}/\text{mL}$  propidium iodide (PI; Sigma, St. Louis, Missouri, USA) and the percentage PI-positive dead cell population was analyzed using a NovoCyte flow cytometer with an FL2 detector. A minimum of 5000 single cells were analyzed per well, and all experiments were performed at least in triplicate.

### *Lipid reactive oxygen species measurement*

Cells were treated with  $5\ \mu\text{M}$  of C11-BODIPY 581/591 (MCE) for 30 minutes at  $37^\circ\text{C}$  in a saturated humidity atmosphere containing 95% air and 5%  $\text{CO}_2$  and then photographed. After that, cells were harvested by trypsinization and resuspended in  $500\ \mu\text{L}$  PBS. Lipid peroxidation was assessed by flow cytometry using a 488 nm laser on an FL1 detector. A minimum of 5000 single cells were analyzed per well.

### *Fe<sup>2+</sup> and malondialdehyde measurement*

Fe<sup>2+</sup> and malondialdehyde (MDA) levels were assayed using commercial kits (ab83366 and ab118970; Abcam, Cambridge, UK).

### *Downstream prediction*

The potential downstream of miR-339 was predicted using an online bioinformatic tool, TargetScan ([https://www.targetscan.org/vert\\_80/](https://www.targetscan.org/vert_80/)).

### *Western blotting*

Total protein was lysed from the cells using radio-immunoprecipitation assay (RIPA) buffer (50 mM Tris pH 8.0, 150 mM NaCl, 1% Triton, 0.1% sodium dodecyl sulphate [SDS], 1 mM ethylenediaminetetraacetic acid [EDTA], 1% sodium deoxycholic acid, 1 mM  $\text{Na}_3\text{VO}_4$ , and 10 mM NaF) with protease inhibitors and phenylmethylsulfonyl fluoride (PMSF). Equivalent amounts of total cellular lysates were separated using 10% SDS-polyacrylamide gel electrophoresis. Primary antibodies used for immunoblotting included anti-ATG7 (1:1000; A2856, Sigma), and antibodies to FTH1 (1:1000; A19544, ABclonal),  $\beta$ -actin (1:10000; AC004, ABclonal). Horseradish peroxidase-conjugated antimouse or antirabbit secondary antibodies (RGAR001 or RGAM001, Proteintech) were used, and signals were determined using Western ECL Substrate. Uncropped data were shown in supplemental material.

### *Cell proliferation assays*

HCCC9810 cells were plated in 6-well plates at a concentration of 10000 cells per well and counted using a Multisizer 3 Coulter Counter (Beckman Coulter, Brea, CA, USA) daily for a week.

### *Statistical analysis*

Results were reported as mean  $\pm$  standard error of the mean (SEM) of 3 or more independent experiments. Statistical analyses were conducted with GraphPad Prism 8.0 software (GraphPad Software, USA). Unpaired Student's *t*-test was used to compare 2 groups, whereas 1-way analysis of variance (ANOVA) was used to compare multiple groups. Statistical significance was defined as  $P < .05$ .

## **Results**

### *miR-339-5p contributes to liver cancer progression*

To investigate the role of miR-339 in liver cancer, we analyzed the mRNA expression level of miR-339 in liver cancer using the TCGA database and found a significant upregulation of miR-339 in liver cancer tissues compared with that in normal tissues (Figure 1A). Moreover, we observed that miR-339 was positively correlated with malignancy in liver cancer (Figure 1B). In addition, its upregulation predicted poor outcomes in patients with liver cancer (Figure 1C). Next, we found that miR-339-5p inhibition significantly suppressed cell proliferation and metastasis in liver cancer cells, as evidenced by the redundant capacity for clone formation and migration (Figure 1D to F). Thus, miR-339 may serve as a potent biomarker for liver cancer.

### *miR-339-5p promotes liver cancer progression by preventing cell death*

To investigate the mechanism through which miR-339-5p promotes the proliferation and metastasis of liver cancer cells,



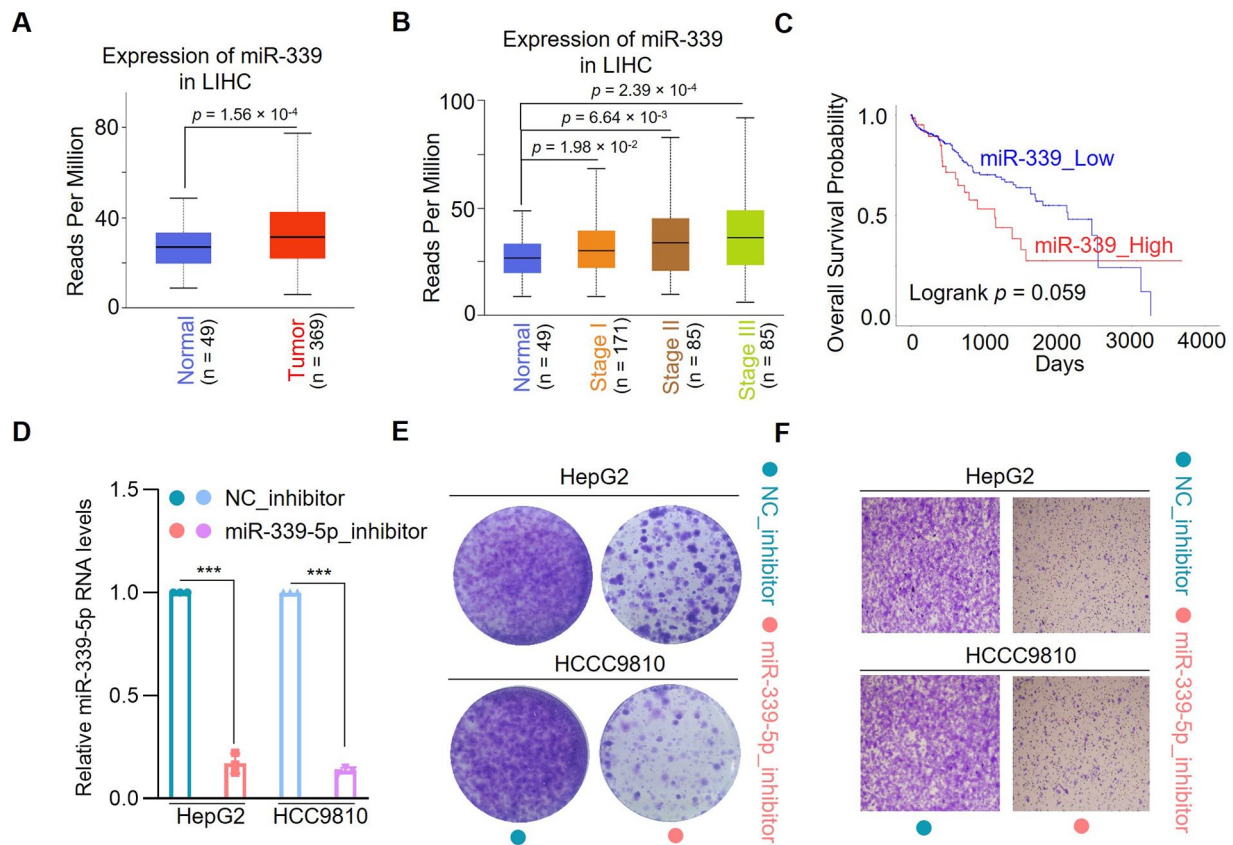


**Figure 1.** miR-339 promotes liver cancer progression. (A) Box plot showing the expression levels of miR-339 in liver cancer samples and paired normal tissues using The Cancer Genome Atlas (TCGA) database. (B) Box plot of the expression in the indicated stages of liver cancer samples analyzed using TCGA database. (C) Kaplan-Meier plot analysis of liver cancer patients with low or high miR-339 expression. (D) The miR-339 knockdown efficiency was determined using real-time quantitative PCR (RT-qPCR). (E) Liver cancer cells expressing NC or miR-339-5p inhibitor were subjected to a colony formation assay. (F) Liver cancer cells expressing NC or miR-339-5p inhibitor were subjected to a transwell migration assay.  $***$ Results with statistical significance were obtained ( $P < .001$ ) through the use of 2-tailed unpaired  $t$ -tests. The data presented in this study represent the mean  $\pm$  SEM from a total of 3 separate experiments.

we examined the effect of miR-339-5p on cell death. miR-339 inhibition significantly induced liver cancer cell death, as seen by cell morphology observation and PI staining (Figure 2A to C). Thus, our data demonstrate that miR-339-5p enhances the ability of liver cancer cells to evade cell death and promote their progression.

#### *miR-339-5p suppresses ferroptosis in liver cancer cells*

Next, we investigated the effect of miR-339 inhibition on cell death. Using inhibitors of various cell death pathways in combination with an miR-339-5p inhibitor, we found that ferroptosis inhibitors could partially rescue cell death caused by miR-339-5p inhibition, indicating that miR-339-5p may inactivate ferroptosis (Figure 3A). Next, we examined intracellular peroxide levels and found that miR-339-5p inhibitor transfection led to the accumulation of intracellular peroxide, MDA, and  $\text{Fe}^{2+}$  (Figure 3B to (D)). Together, these findings suggest that the miR-339-5p inhibitor contributes to cell death, partly through activation of the ferroptosis signaling pathway.

#### *ATG7 serves as the potential downstream target of miR-339*

To investigate how miR-339 limits the sensitivity of liver cancer cells to ferroptosis, we analyzed the possible downstream target genes of miR-339 using the TargetScan database,<sup>29</sup> followed by overlapping with a set of pro-ferroptosis genes using Gene Set Expression Analysis, and identified ATG7 as a potential novel target of miR-339 (Figure 4A). The target region of miR-339 was found in ATG7 as shown in Figure 4B. Consistent with a previous study, ATG7 positively correlated with ferroptosis in liver cancer (Figure 4C). More importantly, we found that the miR-339 inhibitor dramatically elevated the mRNA and protein levels of ATG7 in liver cancer cells (Figure 4D and E). Therefore, we hypothesized that miR-339 inhibited ferroptosis by targeting ATG7.

#### *miR-339 promotes liver cancer progression by targeting ATG7*

To confirm our hypothesis, we silenced ATG7 in cells expressing the miR-339 inhibitor and validated its knockdown efficiency

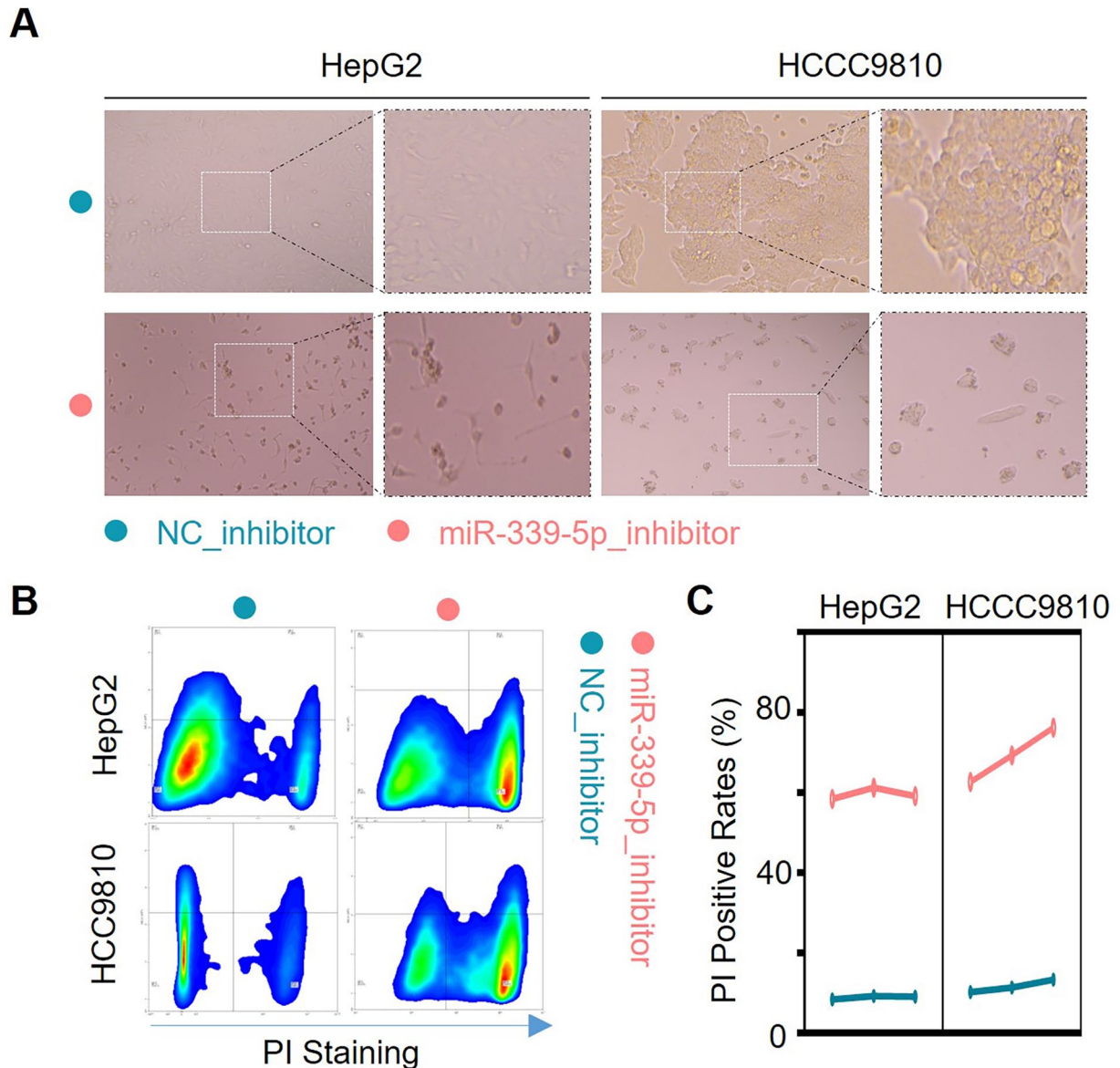


**Figure 2.** miR-339 inhibition leads to cell death in liver cancer cells. (A) Representative morphology of liver cancer cells expressing NC or miR-339 inhibitors. (B and C) Liver cancer cells expressing NC or miR-339 inhibitor were stained with propidium iodide, followed by flow cytometry analysis. Data are presented as mean  $\pm$  SEM of 3 independent experiments.

(Figure 5A). Based on this, we found that the knockdown of ATG7 could rescue cell death caused by the miR-339 inhibitor by observing cell morphology (Figure 5B). These results were confirmed by PI staining (Figure 5C). Furthermore, cell growth and clone formation assays confirmed that ATG7 knockdown rescued the decrease in cell proliferation caused by miR-339 inhibition (Figure 5D and E). Taken together, these results demonstrate that miR-339 suppresses cell death by targeting ATG7, which in turn enhances cell proliferation.

#### *miR-339 promotes ferroptosis resistance in liver cancer by targeting ATG7*

To explore whether miR-339 regulates the sensitivity of liver cancer cells to ferroptosis inducers via ATG7, we examined the

ferroptosis-related indicators following ATG7 knockdown. As seen from the intracellular MDA and lipid peroxidation levels, miR-339 inhibition significantly enhanced the sensitivity of liver cancer cells to the ferroptosis inducer RSL3 compared with the control group (Figure 6A and B). Previous studies have shown that ATG7 regulates ferroptosis through autophagic degradation of FTH1 protein, leading to changes in intracellular iron ion abundance. We next investigated whether miR-339 reduced the sensitivity to RSL3 in liver cancer cells through the ATG7/FTH1 signaling axis. We first examined the intracellular iron ion content and found that the miR-339 inhibitor significantly elevated it compared with that in the control group and that knockdown of ATG7 rescued the increase in intracellular iron ion content caused by the miR-339 inhibitor (Figure 6C). We also examined the protein levels

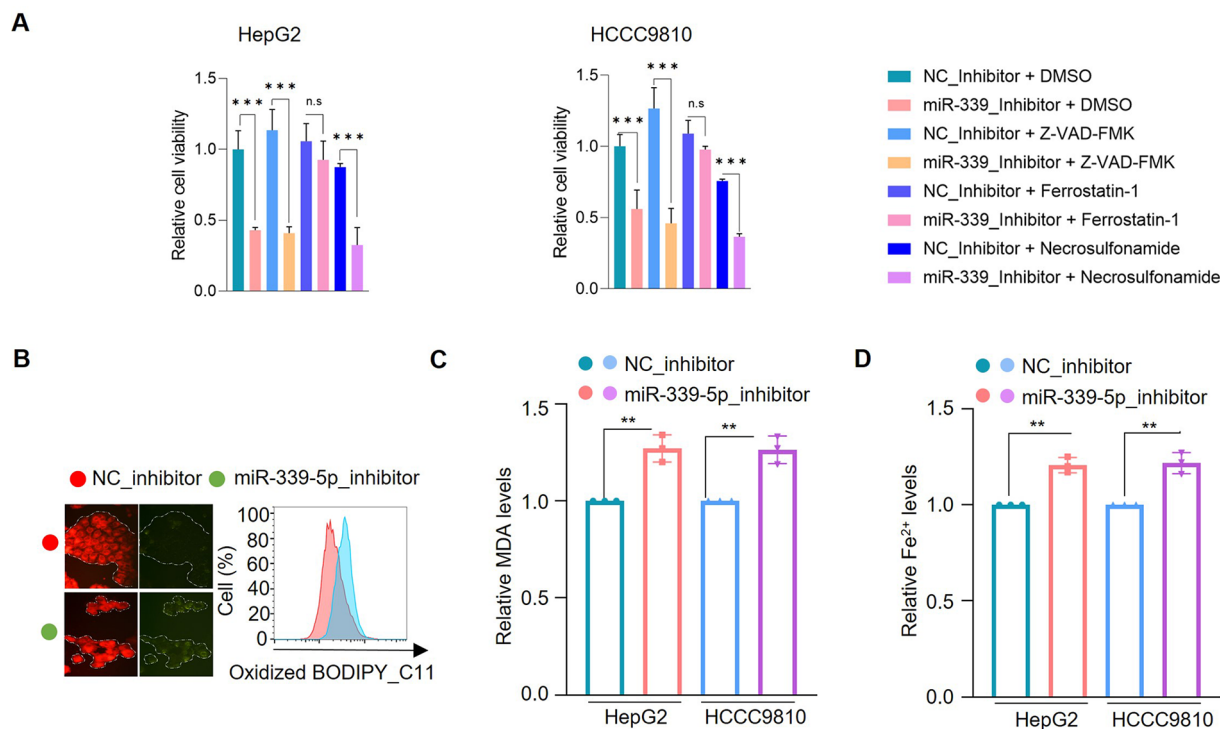


**Figure 3.** Depletion of miR-339 induces ferroptosis in liver cancer cells. (A) Liver cancer cells expressing the miR-339 inhibitor were treated with the indicated inhibitors, and cell viability was determined by the CCK-8 assay. (B) Lipid reactive oxygen species levels were determined by Oxidized BODIPY\_C11 staining. (C) The MDA levels in the HepG2 and HCC9810 cells were determined using an MDA Detection Kit. (D) Cells expressing NC or miR-339 inhibitor were stained with an Fe<sup>2+</sup> probe, visualized by microscopy, and analyzed using ImageJ. The significance level ( $P < .05$ ) was obtained through 2-tailed unpaired  $t$ -tests. The results display the average  $\pm$  standard error of the mean from 3 separate trials.

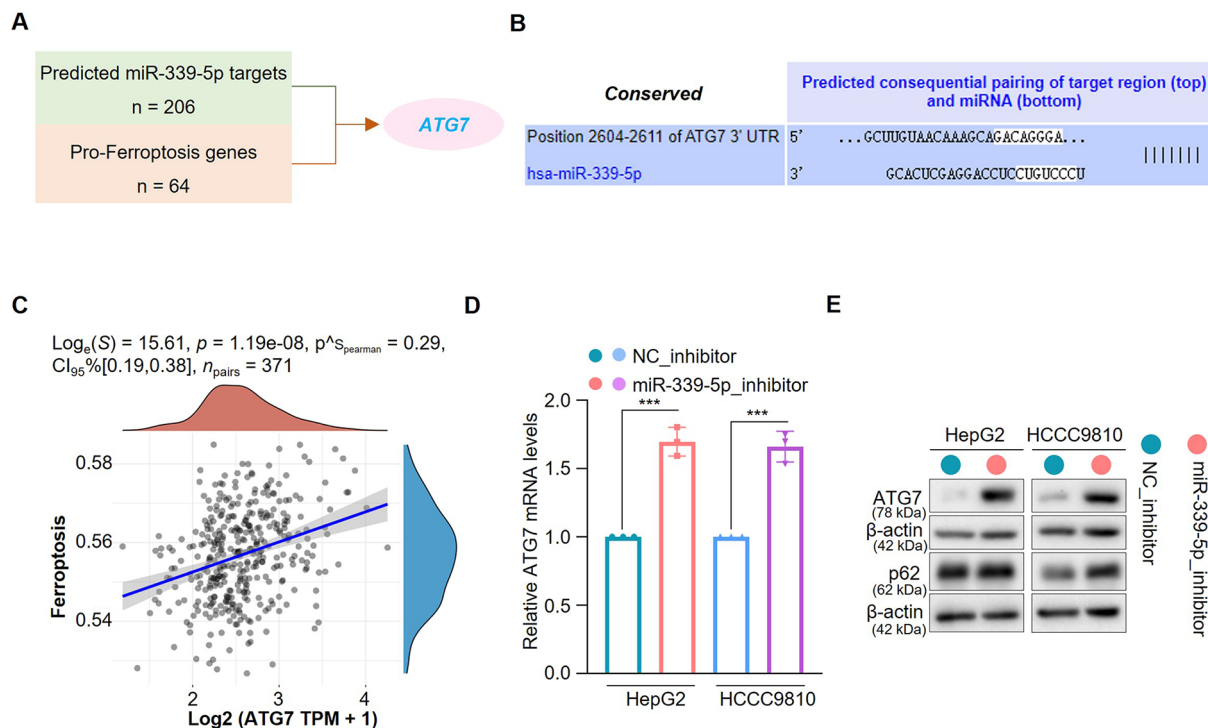


**Figure 4.** miR-339 targets ATG7. (A) Workflow of screening for miR-339 targets. (B) Conserved binding sites of miR-339 in ATG7. (C) Correlation between ATG7 mRNA levels and ferroptosis scores in liver cancer samples was determined using TCGA database. (D and E) Cells expressing NC or the miR-339 inhibitor were subjected to RT-qPCR (D) or IB analysis (E).  $***P < .001$ . The  $P$  values were calculated by conducting 2-tailed unpaired  $t$ -tests. The data were displayed as the average  $\pm$  standard error of the mean from 3 separate trials.



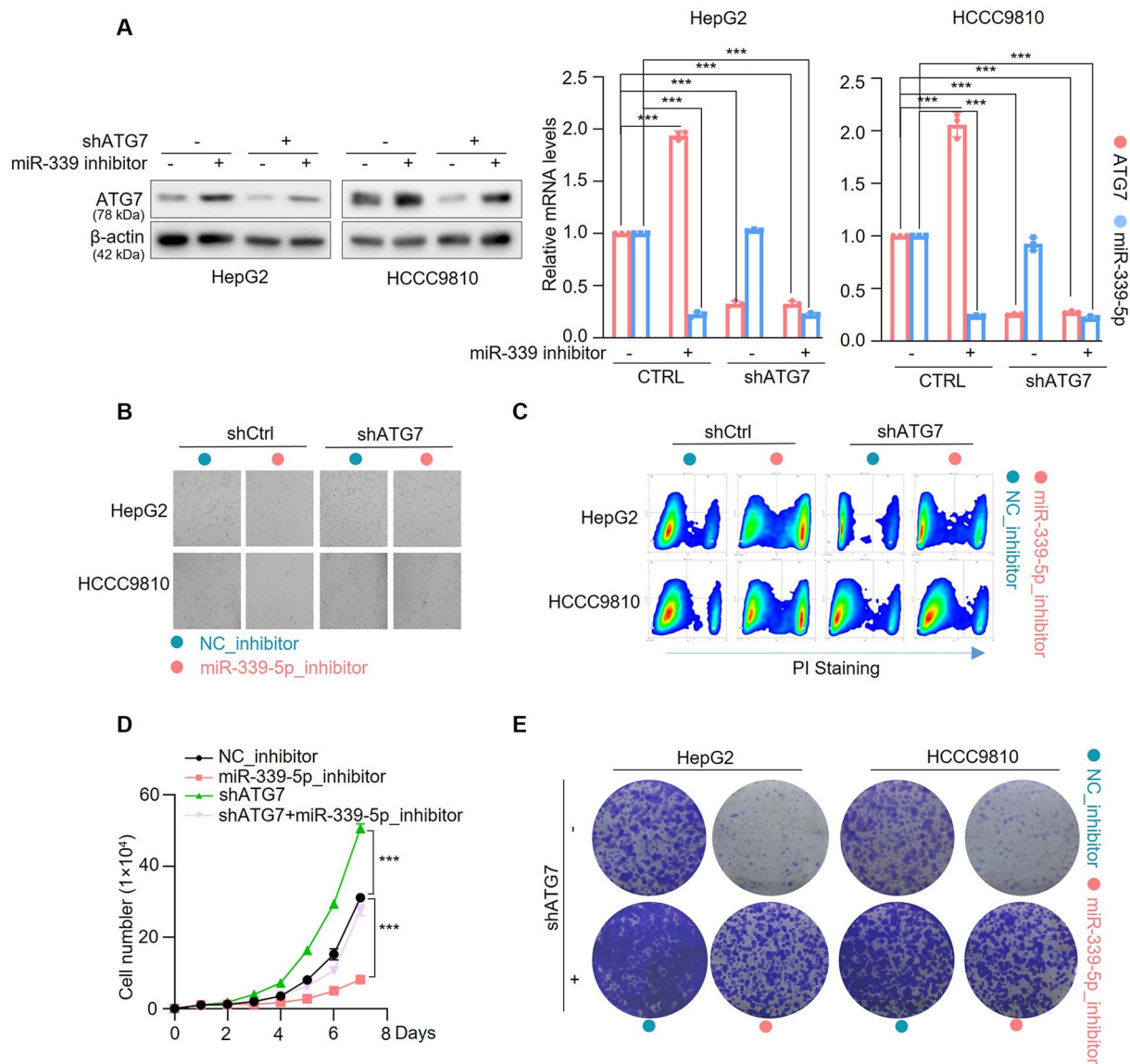


**Figure 5.** Induction of ATG7 contributes to miR-339 inhibition-induced cell death. (A) Cells transfected with the indicated plasmids were subjected to IB and RT-qPCR analyses. (B) Representative morphology of liver cancer cells expressing the indicated plasmids. (C) Liver cancer cells expressing the indicated plasmids were stained with PI, followed by flow cytometry analysis. (D) Growth curve of liver cancer cells expressing the indicated plasmids. (E) Cells expressing the indicated plasmids were subjected to a colony formation assay.  $***P < .001$ . 1-way analysis of variance (ANOVA) was conducted to determine the  $P$  values. Data are presented as mean  $\pm$  SEM of 3 independent experiments.

of intracellular FTH1 and found that miR-339 significantly decreased the protein expression of FTH1, and knockdown of ATG7 partially rescued the decrease in FTH1 protein caused by the miR-339 inhibitor and this alteration pattern was also observed in cells with RSL3 treatment (Figure 6D). Hence, we conclude that in liver cancer cells, miR-339 can lead to the degradation of FTH1 by targeting ATG7, which in turn reduces the sensitivity of cells to ferroptosis inducers.

## Discussion

Early prevention, detection, and intervention are “golden rules” for cancer treatment worldwide.<sup>6,30</sup> However, because of the insidious nature of liver cancer, patients are often already in the middle to late stages of liver cancer when they are diagnosed, and the survival rate of patients with advanced liver cancer is generally poor.<sup>30</sup> The

limited survival benefit of these clinical trials suggests that further research is needed to validate these biomarkers for the surveillance or treatment of liver cancer, and their oncogenic mechanisms are urgently required. Ferroptosis modulates the sensitivity of tumor cells to chemotherapeutic agents, targeted drugs, and immunotherapy, making it a popular subject of research in liver cancer therapy.<sup>7,11,12</sup> By integrating existing studies, it is easy to explore whether epigenetic modification mechanisms are important for understanding liver cancer development, drug resistance, and metastasis.<sup>4,11,31</sup> MicroRNAs, as important components of epigenetic modifications, control the synthesis of more than 60% of the proteins in the body and are essential for tumorigenesis and metastasis.<sup>21,22</sup> The dysregulation of miRNAs in almost all types of cancer has already been demonstrated, and the specific mechanisms underlying their involvement in cancer have been

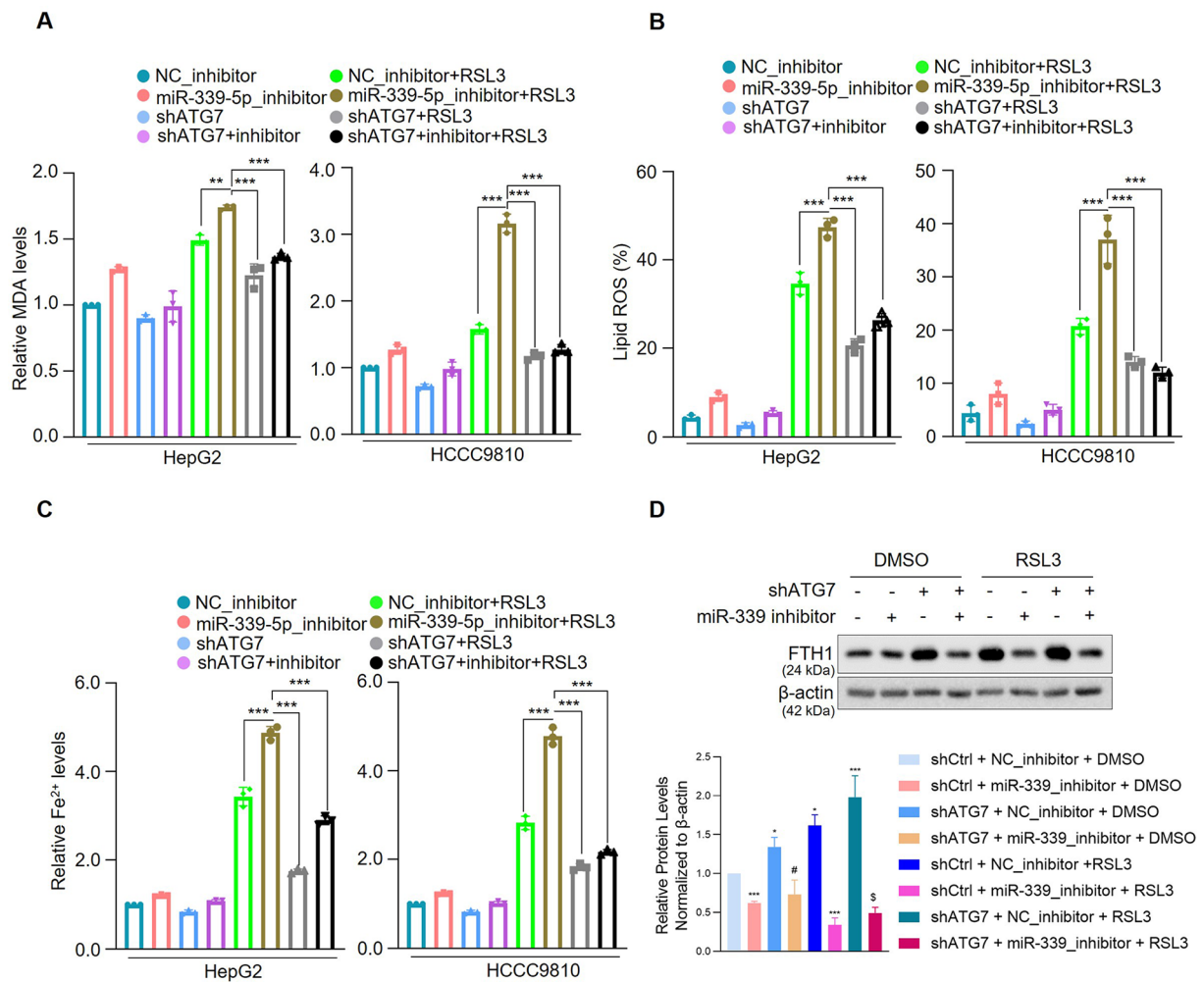


**Figure 6.** miR-339 targets ATG7/FTH1 axis to suppress ferroptosis. (A) Liver cancer cells expressing the indicated plasmids were analyzed using the MDA Detection Kit. (B) Liver cancer cells expressing the indicated plasmids were stained with Oxidized BODIPY\_C11 and analyzed by flow cytometry. (C) Liver cancer cells expressing the indicated plasmids were stained with Fe<sup>2+</sup> probe, visualized by microscopy, and analyzed using ImageJ. (D) FTH1 protein levels in cells were determined by IB analysis. \*\*\* $P < .001$ , compared with shCtrl + NC\_inhibitor + DMSO; # $P < .05$ , compared with shCtrl + miR-339\_inhibitor + DMSO; \$ $P < .05$ , compared with shCtrl + miR-339\_inhibitor + RSL3.  $P$  values were determined using 1-way analysis of variance (ANOVA). Results are displayed as the mean  $\pm$  standard error of the mean (SEM) from 3 separate trials.

revealed.<sup>21,22</sup> More importantly, miRNAs have been suggested to play a role in liver cancer progression.<sup>32,33</sup> However, their regulatory roles in ferroptosis in cancer are not well understood, although there is strong evidence that miRNAs are involved in critical processes in cancer cells. Many drug companies are beginning to explore the role of miRNA-based drugs or miRNA antagonists in cancer therapy, and existing studies suggest that miRNAs may also serve as biomarkers for tumor diagnosis and prognosis.<sup>34,35</sup> Notably, miRNAs are effective nanotherapeutic targets in HCC treatment.<sup>36</sup> In this study, we detected remarkable upregulation of miR-339 in liver cancer cells. Our results further indicated that miR-339 may promote liver cancer progression by inhibiting ferroptosis. Collectively, our study not only identified predictive and nanotherapeutic targets for liver cancer, but also elucidated their oncogenic mechanisms, making it possible to target ferroptosis in liver cancer.

Cellular autophagy can regulate ferroptosis through non-classical pathways.<sup>17</sup> MicroRNAs directly or indirectly regulate

cellular autophagy<sup>28</sup> and ferroptosis.<sup>27</sup> However, the upstream mechanism by which autophagy affects ferroptosis remains exclusive. Here, we demonstrated that miR-339, which is highly expressed in liver cancer, rendered tumor cells resistant to cell death by inhibiting ferroptosis. Mechanistically, we provided substantial evidence to verify that miR-339 can regulate the sensitivity of liver cancer cells to ferroptosis inducers by targeting ATG7, causing autophagic degradation of the FTH1 protein, thereby regulating cell proliferation and metastasis. This is due to its crucial role in ferroptosis and HCC development. Further in-depth analyses are required to confirm the role of miR-339 in liver cancer and ferroptosis.

### Limitations

There was a contradict about the diametrically opposed trends in the correlation analysis about the correlation between miR-339 expression and malignancies of LIHC. We found that the patient samples under investigation are from different ethnic



groups.<sup>37</sup> Noticeably, the same genes are expressed differently in different races due to genetic backgrounds and environments and may exert different regulatory functions.<sup>38</sup> We therefore speculated that there might be a difference here due to ethnic differences. Also, this contradict suggests that we need to collect more clinical samples to validate the relationship between miR-339 expression and liver cancer malignancies to further support the role of miR-339 as a biomarker for liver cancer. In addition, we do not have the condition to perform in vivo study which results in the inadequate support for therapeutic role of miR-339 in liver cancer.

## Conclusions

This study provides important evidence that the miR-339 inhibition activates of the autophagy pathway to promote ferroptosis by degrading FTH1 in liver cancer cells. Taken together, our results suggested that targeting miR-339 may be an effective strategy for developing HCC interventions.

## Acknowledgements

The results shown in Figure 1A to C and Figure 4C are based on data generated by the TCGA Research Network (<https://www.cancer.gov/tcga>).

## Author Contributions

JZ designed the study; FC, WH, and WL performed most of the experiments; HZ performed the related bioinformatics analyses. FC analyzed the data; JZ and FC wrote the manuscript.

## Availability of Data and Materials

All the data or materials can be acquired from corresponding author by a reasonable request.

## ORCID iD

Jiaping Zheng  <https://orcid.org/0000-0003-0367-9250>

## Supplemental Material

Supplemental material for this article is available online.

## REFERENCES

- Llovet JM, De Baere T, Kulik L, et al. Locoregional therapies in the era of molecular and immune treatments for hepatocellular carcinoma. *Nat Rev Gastroenterol Hepatol.* 2021;18:293-313.
- Yang JD, Hainaut P, Gores GJ, Amadou A, Plymoth A, Roberts LR. A global view of hepatocellular carcinoma: trends, risk, prevention and management. *Nat Rev Gastroenterol Hepatol.* 2019;16:589-604.
- Kim E, Viatour P. Hepatocellular carcinoma: old friends and new tricks. *Exp Mol Med.* 2020;52:1898-1907.
- Yang C, Zhang H, Zhang L, et al. Evolving therapeutic landscape of advanced hepatocellular carcinoma. *Nat Rev Gastroenterol Hepatol.* 2023;20:203-222.
- Yao F, Deng Y, Zhao Y, et al. A targetable LIFR-NF-kappaB-LCN2 axis controls liver tumorigenesis and vulnerability to ferroptosis. *Nat Commun.* 2021;12:7333.
- Llovet JM, Kelley RK, Villanueva A, et al. Hepatocellular carcinoma. *Nat Rev Dis Primers.* 2021;7:6.
- Gong D, Chen M, Wang Y, Shi J, Hou Y. Role of ferroptosis on tumor progression and immunotherapy. *Cell Death Discov.* 2022;8:427.
- Dixon SJ, Lemberg KM, Lamprecht MR, et al. Ferroptosis: an iron-dependent form of nonapoptotic cell death. *Cell.* 2012;149:1060-1072.
- Chen X, Kang R, Kroemer G, Tang D. Broadening horizons: the role of ferroptosis in cancer. *Nat Rev Clin Oncol.* 2021;18:280-296.
- Jiang X, Stockwell BR, Conrad M. Ferroptosis: mechanisms, biology and role in disease. *Nat Rev Mol Cell Biol.* 2021;22:266-282.
- Lei G, Zhuang L, Gan B. Targeting ferroptosis as a vulnerability in cancer. *Nat Rev Cancer.* 2022;22:381-396.
- Du Y, Guo Z. Recent progress in ferroptosis: inducers and inhibitors. *Cell Death Discov.* 2022;8:501.
- Sun X, Niu X, Chen R, et al. Metallothionein-1G facilitates sorafenib resistance through inhibition of ferroptosis. *Hepatology.* 2016;64:488-500.
- Ajoolabady A, Tang D, Kroemer G, Ren J. Ferroptosis in hepatocellular carcinoma: mechanisms and targeted therapy. *Br J Cancer.* 2023;128:190-205.
- Debnath J, Gammoh N, Ryan KM. Autophagy and autophagy-related pathways in cancer. *Nat Rev Mol Cell Biol.* 2023;24:560-575.
- Yamamoto H, Zhang S, Mizushima N. Autophagy genes in biology and disease. *Nat Rev Genet.* 2023;24:382-400.
- Hou W, Xie Y, Song X, et al. Autophagy promotes ferroptosis by degradation of ferritin. *Autophagy.* 2016;12:1425-1428.
- Wang N, Ma T, Yu B. Targeting epigenetic regulators to overcome drug resistance in cancers. *Signal Transduct Target Ther.* 2023;8:69.
- Vasudevan S, Tong Y, Steitz JA. Switching from repression to activation: microRNAs can up-regulate translation. *Science.* 2007;318:1931-1934.
- Trino S, Lamorte D, Caivano A, et al. MicroRNAs as new biomarkers for diagnosis and prognosis, and as potential therapeutic targets in acute myeloid leukemia. *Int J Mol Sci.* 2018;19:460.
- Weiss CN, Ito K. A macro view of microRNAs: the discovery of microRNAs and their role in hematopoiesis and hematologic disease. *Int Rev Cell Mol Biol.* 2017;334:99-175.
- Yang I-P, Yip K-L, Chang Y-T, et al. MicroRNAs as predictive biomarkers in patients with colorectal cancer receiving chemotherapy or chemoradiotherapy: a narrative literature review. *Cancers.* 2023;15:1358.
- Bandiera S, Pfeffer S, Baumert TF, Zeisel MB. miR-122—a key factor and therapeutic target in liver disease. *J Hepatol.* 2015;62:448-457.
- Wu ZS, Wu Q, Wang C-Q, et al. MiR-339-5p inhibits breast cancer cell migration and invasion in vitro and may be a potential biomarker for breast cancer prognosis. *BMC Cancer.* 2010;10:542.
- Zhou C, Liu G, Wang L, et al. MiR-339-5p regulates the growth, colony formation and metastasis of colorectal cancer cells by targeting PRL-1. *PLoS ONE.* 2013;8:e63142.
- Shen B, Zhang Y, Yu S, et al. MicroRNA-339, an epigenetic modulating target is involved in human gastric carcinogenesis through targeting NOVA1. *FEBS Lett.* 2015;589:3205-3211.
- Zhang N, Huang J, Xu M, Wang Y. LncRNA T-UCR Uc.339/miR-339/SLC7A11 axis regulates the metastasis of ferroptosis-induced lung adenocarcinoma. *J Cancer.* 2022;13:1945-1957.
- Li G and Cheng Z. miR-339-5p inhibits autophagy to reduce the resistance of laryngeal carcinoma on cisplatin via targeting TAK1. *Biomed Res Int.* 2021;2021:9938515.
- McGeary SE, Lin KS, Shi CY, et al. The biochemical basis of microRNA targeting efficacy. *Science.* 2019;366:eav1741.
- An L, Zheng R, Zhang S, et al. Hepatocellular carcinoma and intrahepatic cholangiocarcinoma incidence between 2006 and 2015 in China: estimates based on data from 188 population-based cancer registries. *Hepatobiliary Surg Nutr.* 2023;12:45-55.
- Wu YL, Lin Z-J, Li C-C, et al. Epigenetic regulation in metabolic diseases: mechanisms and advances in clinical study. *Signal Transduct Target Ther.* 2023;8:98.
- Mo Z, Li R, Cao C, et al. Splicing factor SNRPA associated with microvascular invasion promotes hepatocellular carcinoma metastasis through activating NOTCH1/Snai1 pathway and is mediated by circSEC62/miR-625-5p axis. *Environ Toxicol.* 2023;38:1022-1037.
- Zhai H, Zhong S, Wu R, et al. Suppressing circIDE/miR-19b-3p/RBMS1 axis exhibits promoting-tumour activity through upregulating GPX4 to diminish ferroptosis in hepatocellular carcinoma. *Epigenetics.* 2023;18:2192438.
- Nascimento LRD, Domingueti CP. MicroRNAs: new biomarkers and promising therapeutic targets for diabetic kidney disease. *J Bras Nefrol.* 2019;41:412-422.
- Peng Y, Croce CM. The role of microRNAs in human cancer. *Signal Transduct Target Ther.* 2016;1:15004.
- Meng H, Li R, Xie Y, et al. Nanoparticles mediated circROBO1 silencing to inhibit hepatocellular carcinoma progression by modulating miR-130a-5p/CCNT2 axis. *Int J Nanomedicine.* 2023;18:1677-1693.
- Wang YL, Chen CM, Wang XM, Wang L. Effects of miR-339-5p on invasion and prognosis of hepatocellular carcinoma. *Clin Res Hepatol Gastroenterol.* 2016;40:51-56.
- Couzin J. Human genetics. In Asians and whites, gene expression varies by race. *Science.* 2007;315:173-174.